 doi:10.20944/preprints202005.0389.v1

# *Candidatus* Liberibacter asiaticus manipulates the expression of vitellogenin, cytoskeleton, and endocytotic pathway-related genes to become circulative in its vector, *Diaphorina citri* (Hemiptera: Psyllidae)

**Running title:** Transcriptomic response of Asian citrus psyllid to *huanglongbing*

Damini Jaiswal[1], V. Kavi Sidharthan[1], Susheel Kumar Sharma[2], Richa Rai[1], Nandlal Choudhary[3], Amalendu Ghosh[1]*, Virendra Kumar Baranwal[1]

[1]Advanced Centre for Plant Virology, ICAR-Indian Agricultural Research Institute, New Delhi 110012, India
[2]ICAR-Research Complex for NEH Region, Manipur Centre, Imphal 795004, India
[3]Amity Institute of Virology and Immunology, Amity University, Sector-125, Noida 201313, India
*Corresponding author's email: amal4ento@gmail.com, ORCID iD: 0000-0001-6634-5771

**Abstract**

BACKGROUND

Citrus greening disease or *huanglongbing* (HLB) caused by *Candidatus* Liberibacter asiaticus (CLas) limits the citrus production worldwide. CLas is transmitted by the Asian citrus psyllid (ACP), *Diaphorina citri* (Hemiptera: Psyllidae) in a persistent-propagative manner. Application of insecticides to manage the psyllid vectors and disease is the most common practice. Understanding the molecular interaction between CLas and ACP and interrupting the interrelationship can provide an alternative to insecticides for managing citrus greening disease.

RESULTS

Transcriptome analysis of ACP in response to CLas showed differential expression of 3911 genes (2196 up-regulated, and 1715 down-regulated) including the key genes of ACP involved in cytoskeleton synthesis and nutrition-related proteins. Majority of the differentially expressed genes were categorized under molecular function followed by cellular components and biological processes. KEGG pathway analysis showed differential regulation of carbohydrate, nucleotide and energy metabolic pathways, the endocytotic pathway and the defense-related pathways. Differential regulation of genes associated with the key pathways might favors CLas to become systemic and propagate in its insect vector.

CONCLUSION

The study provides an understanding of genes involved in circulation of CLas in ACP. The candidate genes involved in key physiological processes and CLas transmission by ACP would be potential targets for sustainable management of ACP and CLas.

**Keywords:** Asian citrus psyllid, citrus greening bacterium, *huanglongbing*, transcriptomics, virus-vector relationship, vitellogenin, cytoskeleton**,** endocytotic pathway

 doi:10.20944/preprints202005.0389.v1

## 1 Introduction

Citrus greening disease, also known as *huanglongbing* (HLB) is a major limiting factor in citrus cultivation worldwide. The disease is incited by a fastidious, phloem-limited, α proteobacterium *Candidatus* Liberibacter. Three species *viz*. *Candidatus* Liberibacter asiaticus (CLas), *C.* L. africanus (CLaf) and *C.* L. americanus (CLam) are reported to be associated with the disease.[1-3] Among them, CLas is the most widespread destroying about 100 million citrus trees in Asia.[2] Infection of *C.* L. spp. produces yellow shoots, leaves with blotchy mottles, and small lopsided fruits. *C.* L. spp. are transported both upward and downward through the tree but their distribution is patchy. The infected branches start to die back and the infected tree dries up gradually. CLas and CLam are transmitted by Asian citrus psyllid (ACP, *Diaphorina citri* Kuwayama, Hemiptera: Psyllidae), whereas African citrus psyllid, *Trioza erytreae* (Del Guercio) is the primary vector of CLaf in Africa. These two psyllids are the only known etiologic agent of HLB and economic psyllid species on citrus in the world. ACP is thought to be originated in Asia, but it is also prevalent in parts of the Middle East, South and Central America, Mexico and the Caribbean. The relationship of *C.* L. spp. with psyllids is a persistent-propagative type and there is evidence of transovarial transmission of *Candidatus* Liberibacter spp. by ACP.[4] CLas is acquired by ACP from infected citrus plants during nymphal or adult stages and carried in the hemolymph and salivary glands of psyllid. The infected ACP provides CLas an entry to phloem of a healthy citrus plant during feeding sap.

The primary strategy for management of HLB is to restrict the psyllid vectors. Application of insecticides is widely adopted to manage psyllid that exerts detrimental effects on the environment and non-target organisms. Development of insecticide resistance in psyllids brings more complexity in the management of HLB. Understanding the intricate relationship of ACP with CLas may open up new novel targets to manage the disease by interrupting the interrelationship. In recent years, transcriptomics has emerged as a promising approach to study the global differential gene expression and also serves as a platform for gene discovery by facilitating comparative genomics. Antennal and abdominal transcriptome of ACP has helped to identify the potential chemosensory proteins.[5] The differentially expressed transcripts of ACP in response to CLas may facilitate to identify putative genes involved in the transmission mechanism. In the present experiment, a transcriptome-wide response of ACP to CLas infection has been reported and expression of few highly regulated genes has been validated. This knowledge may be useful in future studies to identify potential molecular targets to interfere with CLas transmission by ACP and management of the disease.

## 2 Materials and methods

### 2.1 Establishing a homogeneous population of ACP, sample preparation and RNA isolation

The initial population of ACP was collected from the experimental field of Indian Agricultural Research Institute (IARI), New Delhi. A homogeneous population of ACP has been established on *Murraya koenigii* plant from a single female. The population was maintained in controlled conditions at 25±2 °C, 60±10% RH, and 8 h dark. Eggs were collected from the homogeneous population with a fine Camel hairbrush. Eggs were placed on healthy and CLas-infected citrus plants separately and reared up to the adult stage. The infection status of plants and psyllids was tested in PCR using OmpCLas primers[6] and DNA isolated from plants and psyllids respectively as templates. Total DNA was isolated from citrus plants and ACP using GeneJet Plant Genomic DNA Purification Mini Kit (Thermo Fisher Scientific, MA, USA), and DNeasy Blood and Tissue kit (Qiagen, Hilden, Germany), respectively following manufacturers' protocol. PCR was performed in 25µl

Preprints (www.preprints.org) | NOT PEER-REVIEWED | Posted: 24 May 2020 doi:10.20944/preprints202005.0389.v1

reaction mixture with 1x PCR buffer containing: 0.5 µM of each forward and reverse primers, 0.5 mM of dNTPs, 50 ng of template DNA and 1 unit of DyNAzyme II DNA polymerase (Thermo Fisher Scientific, MA, USA). The PCR conditions of 3 min of initial denaturation at 94°C, followed by 35 cycles of 30 s of denaturation at 94°C, 30 s of annealing at 52°C, 45 s of extension at 72°C, and a single final extension of 10 min at 72°C were used. PCR products were resolved on 1.6% agarose gel containing ethidium bromide and visualized in a UV illuminator.

Two sets of CLas-infected adult psyllids (designated as P+CLas1 and P+CLas2) and one set of healthy adult psyllid (designated as P-CLas) were subjected to total RNA isolation using TRIzol (Invitrogen) following manufacturer's protocol. RNA concentration and quality were assessed using standard procedures as recommended for Illumina (Illumina, San Diego, CA, USA) sequencing. Another set of samples (both P+CLas, P-CLas) obtained from the same batch were preserved in -80ºC for qRT-PCR experiments.

**2.2 Library preparation and sequencing**

In brief, 500 ng of total RNA was used to enrich mRNA using NEB Magnetic mRNA Isolation Kit. The transcriptome library was prepared using NEB ultraII RNA library prep kit and sequenced using Illumina Next Seq 500 paired-end technology. The enriched mRNA was fragmented (approximately 200 bp) using a fragmentation buffer. Random hexamer primers were then added and hybridized to complementary RNA sequences. These short fragments were used as templates to synthesize the first-strand cDNA using reverse transcriptase and dNTPs. The DNA-RNA hybrids synthesized during first-strand cDNA synthesis were converted into full-length double-stranded cDNA using RNase H and *E. coli* DNA polymerase I and then second-strand cDNA was synthesized using second strand enzyme mix and buffer. The double-stranded cDNA fragments were purified using 1.8X Ampure beads. The purified double-stranded cDNA was end-repaired to ensure that each molecule was free of overhangs and had 5′ phosphates and 3′ hydroxyls before the adaptor ligation. The adaptor-ligated DNA was purified using Ampure beads and was enriched using specific primers, compatible with sequencing on to the Illumina platforms. The final enriched library was purified and quantified by Qubit and the size was analyzed by Bioanalyzer.

**2.3 Pre-processing of raw reads and differential gene expression analysis**

The quality of raw reads was visualized using FASTQC v0.11.2. Raw reads were pre-processed by removing the adaptor sequences, duplicated sequences, ambiguous and low-quality reads to obtain high-quality reads. After pre-processing, the quality of reads was ensured again using FASTQC. Pre-processed reads were mapped to the reference genome of *D. citri* (GCF_000475195.1) using TopHat v2.1.0 software with default parameters except for the mismatch parameter that was set to two. Gene expression was quantified using Subread v1.5.0 software with default parameters based on the Fragments Per Kilobase of transcript sequence per Millions base pairs-sequenced (FPKM values). Average FPKM value of expressed genes from two P+CLas samples (designated as combined P+CLas) was compared with FPKM value of expressed genes of P-CLas sample for identification of differentially expresses genes (DEGs) using edgeR v1.24.0 software (without biological replicates). Genes having a normalized P-value <0.05 were only considered for differential expression analysis. Genes with FPKM values >1 and <-1 were regarded as up and down-regulated, respectively. GO enrichment analysis of DEGs was performed (corrected p-value <0.05) using a web-based tool AgriGO.[7] KEGG pathway enrichment analysis of

Preprints (www.preprints.org) | NOT PEER-REVIEWED | Posted: 24 May 2020 doi:10.20944/preprints202005.0389.v1

DEGs was performed to identify the pathways that were differentially regulated between combined P+CLas and P-CLas samples using the software KOBAS v3.0 with corrected p-value <0.05.

### 2.4 Quantitative real time-PCR (qRT-PCR) analysis

To validate a few most differentially regulated genes (vitellogenin-1, vitellogenin-2, troponin C and tropomyosin-1) of ACP, the top two genes each from up- and down-regulated were selected. QRT-PCR analysis was performed in Insta Q 48m (Himedia) using the Maxima SYBR Green/ROX qPCR Master Mix (Thermo Fisher Scientific). *α- tubulin* was used as a reference for normalization of gene expression.[8] Firstly, total RNA was isolated from P-CLas and P+CLas psyllid samples stored in -80ºC using ZR Tissue and Insect RNA MicroPrep (ZymoResearch, California, USA). DNase treatment was performed using DNase I (Thermo Fisher Scientific, MA, USA) following the manufacturer's protocol. First-strand of cDNAs were synthesized with Oligo(dT)$_{12-18}$ primer using First-strand cDNA synthesis kit (Thermo Fisher Scientific) following manufacturer's instructions. Primers were designed for the target genes using the web-based Primer3 Input (https:// frodo.wi.mit.edu/). The primer sequences used in this study are listed in Table 1. The 30 µl qRT-PCR reaction mixture consisted of 2 µl of cDNA, 0.5 µl of 10 µM forward and reverse primers each, 12.5 µl of SYBR Green master mix and 14.5 µl of nuclease-free water. Following thermal cycling was followed, initial denaturation at 94ºC for 3 min, then 30 cycles of 94 ºC for 30s, 62 ºC for 30s and 72 ºC for 30s followed by a melting stage. Each reaction including a non-template control was replicated thrice. The relative gene expression was calculated using the $2^{-\Delta\Delta CT}$ method.[9] Statistical significance of the qRT-PCR data was analyzed using Tukey's multiple comparison tests. Values with $p < 0.05$ were considered to be statistically significant.

## 3 Results

### 3.1 CLas infection in ACP and citrus plant

PCR with CLas-infected citrus plant and ACP yielded corresponding amplification of 809 bp in agarose gel electrophoresis. No amplification was observed in the case of CLas-free citrus plant and ACP exposed to healthy citrus plants.

### 3.2 Pre-processing of raw data and mapping of clean reads to reference genome

Raw reads obtained from three libraries (P+CLas1, 2 and P-CLas) ranged from 63.96 to 77.18 million with an average of 68.82 million. 98.93% to 99.21% of the total raw reads in three libraries qualified as clean reads after pre-processing steps. The proportion of clean reads that mapped to ACP genome ranged from 62.8% to 48.4% across libraries with an average of 58.7%. Among the mapped reads, 39.2% to 47.5% of the total reads were uniquely mapped while 9.2% to 15.3% of the total reads were mapped to multiple loci in the genome (Table 2).

### 3.3 Global gene expression analysis

Genes having FPKM values greater than or equal to 1 were considered to be expressed. A total of 17,437 and 17,059 expressed genes were found in P+CLas1 and P+CLas2 samples, respectively while 15,444 genes were expressed in P-CLas. In DEG analysis using edgeR with BH correction, a heatmap of significantly expressed genes was generated. It was observed that the P+CLas samples clustered together as their gene expression

patterns were nearly similar. However, both the samples differed from P-CLas indicating their differential gene expression pattern from the later (Fig. 1).

**3.4 Differential gene expression analysis**

In total, 3911 genes (27%) were found to be differentially expressed between combined P+CLas and P-CLas samples while the expression of 73% of the genes remained unaltered (Fig. 2A). Among the DEGs, 2196 and 1715 genes were up-regulated and down-regulated respectively in combined P+CLas as compared to P-CLas (Fig. 2B). The top 20 differentially expressed (up and down-regulated) genes in CLas-infected ACP have been listed in Table 3. Nutrition-related genes of ACP like vitellogenin-1, -2, and -3, and extensin were found highly overexpressed post exposure to CLas. Significant downregulation of cytoskeleton-related genes of ACP such as myosin heavy chain, troponin C, tropomyosin-1, E3 ubiquitin, and flightin was also recorded. In addition, few genes possibly involved in CLas-ACP interaction were differentially expressed such as laminin, papilin, integrin, talin, phenoloxidase, serine proteases, hemocytin, cathepsin B, and ABC transporters.

**3.5 Functional analysis of DEGs**

Gene Ontology (GO) terms were assigned to the 3911 DEGs. Based on the GO terms, DEGs were broadly grouped into three categories *viz*. genes associated with cellular components, biological processes, and molecular functions. The majority of the DEGs were categorized under molecular functions (50%) followed by cellular components (33%) and biological processes (17%) (Fig. 3A). In molecular function category, genes associated with catalytic activity, binding and nucleotide-binding were mostly enriched. Genes associated with cell, cell parts, membrane sub-categories were differentially enriched in cellular component category. In the biological processes, genes associated with metabolic, cellular and primary metabolic processes were the most enriched (Fig. 3B). Fig. 4 shows the highly enriched molecular functions in CLas-infected ACP.

**3.6 KEGG pathway analysis of DEGs**

Based on the KEGG pathway analysis, the DEGs were involved in metabolism, environmental and nucleotide signal processing, organismal systems and cellular processes. The major metabolic pathways affected include carbohydrate, nucleotide, and energy metabolism while transcription, translation, folding, sorting and degradation were the differentially regulated nucleotide signal processing pathways. Genes involved in signal transduction and aging that aid in environmental signal processing and organismal systems respectively were also differentially regulated. Transport and catabolism related pathways remained the most affected cellular processes (Fig. 5). The results of KEGG pathway analysis were consistent with the pathways identified in GO enrichment analysis.

**3.7 Validation of DEGs in qRT-PCR**

Expression of vitellogenin-1 and vitellogenin-2 genes was 8.0 and 8.4-fold higher respectively in P+CLas sample as compared to P-CLas. However, troponin C and tropomyosin-1 genes were down-regulated to 6.0 and 5.4-fold respectively in P+CLas sample in comparison with P-CLas samples. Similarly, RNA-seq analysis showed that expression of vitellogenin-1 and vitellogenin-2 genes were up-regulated to 18.4 and 17.0-fold respectively while the troponin C and tropomyosin-1 genes were down-regulated to 5.8 and 5.0-fold

 doi:10.20944/preprints202005.0389.v1

respectively in CLas-infected ACP samples (Fig. 6). Melt curve analysis in qRT-PCR confirmed the specificity of the reactions.

**4 Discussion**

A host-pathogen-vector relationship involves complex direct and indirect interactions where pathogen and vector compete with each other for a shared host. They can affect each other by altering the biochemical traits of the host. A hypothesis of the manipulation of vectors by the pathogens has been proposed by Ingwell et al.[10] This could occur by modifying the physiological processes of the vector directly.[11,12] Both positive and negative effects of plant pathogens on their vectors have been recorded.[12-14] CLas is transmitted by ACP in a persistent-propagative manner.[4] Multiplication of CLas in ACP suggests a potential alteration in the physiological process of ACP. ACP nymphs acquire CLas from infected hosts efficiently than the adults and become viruliferous in late instars or after emergence as adults. ACP adults can also acquire the virus in 15-30 min feeding on infected host plants but an increase in titer of CLas was found when acquired by nymphs.[15] Once acquired, CLas crosses the mid-gut barrier and reaches hemolymph of ACP. It is thought to be transported to the salivary gland and accumulates there to infect healthy hosts during feeding and salivation. CLas also invades reproductive organ of ACP and carried to the next generation through eggs.[4] The molecular mechanism of interaction between ACP and CLas is still unknown. Transcriptomic studies have been used to understand the interaction between pathogen and vector at the molecular level.[15] The present study was performed to understand the differential gene expression pattern in ACP in response to CLas infection. Cluster analysis of expressed genes grouped the two sets of ACP samples infected with CLas and both these samples were different from the healthy ACP sample indicating the differential gene expression pattern between CLas-infected and CLas-free psyllids.

A group of vitellogenin genes of ACP was found upregulated post CLas exposure in the current study. Vitellogenin proteins are the major egg yolk protein precursors in insects.[15] However, the expression of vitellogenin gene in honey bee males suggests their possible role other than yolk formation.[16] Role of vitellogenins as antioxidants in honey bees and *Caenorhabditis elegans*[17,18] and as antibacterial agents in *Bombyx mori*[19] has been elucidated. Recently, Huo et al.[20] uncovered a positive correlation between the presence of vitellogenin and in-hemolymph survival of rice stripe virus (RSV) in *Laodelphax striatellus.* The study showed that vitellogenin interacted with RSV to protect the latter in the unhostile hemolymph environment of *L. striatellus.* The upregulation of vitellogenin-like genes in the current study, thus, suggests the putative role of these proteins in protecting CLas in the hemolymph of ACP for the earlier to systemically colonize various tissues of the insect vector. In addition, extensin-like proteins that are involved in pathogenic stress response in insects[21] were upregulated in CLas infected ACP. Laminin, one of the major constituents of the midgut and salivary gland basal lamina, functions as receptors for parasites in invertebrate systems.[22] The upregulation of laminin gene in CLas-infected ACP suggests it's possible to bind with basal lamina to cross the midgut and salivary gland barriers.

Genes like tropomyosin and troponin C of ACP have been recorded to be downregulated post exposure to CLas. Tropomyosins are evolutionally conserved proteins that bind to the actin filaments and participate in a range of cellular processes. In insects, tropomyosin in collaboration with the troponin complex regulates skeletal muscle contraction and relaxation thereby playing an important role in regulation of insect survival, feeding, and

 doi:10.20944/preprints202005.0389.v1

breeding.[23] In a recent study, Lan et al.[24] showed that rice dwarf virus (RDV) reduced the survival and fecundity of its vector, *Nephotettix cincticeps* by downregulating the expression of troponin C. Similarly, CLas infection of ACP was shown to downregulate the cytoskeletal proteins to induce changes in cytoskeletal configuration.[25] Downregulation of troponin C and tropomyosin-1 genes in CLas-infected ACP in the current study also suggests the possible cytoskeletal modification in cells of ACP to mediate the circulation of CLas within ACP. In addition, flightin, a myosin-binding protein that facilitates thick filament assembly and muscle integrity,[26] also showed reduced expression in CLas-infected ACP. Taken together, all these might account for the morphological abnormalities of the CLas-infected ACP as demonstrated by Ghanim et al. (2016).[27] Downregulation of enzymes like E3 ubiquitin ligase suggests the possible manipulation of 26S proteasomal degradation pathway of ACP by CLas to prevent proteins of the later from degradation.[25] Similarly, downregulation of defense-related genes like phenoloxidase enzyme involved in melanization, proteins involved in insect humoral responses- serine proteases, hemocytin, and cathepsin B, a proteolytic enzyme, associated with insect stress suggests the subversion of ACP's defense by CLas. ABC transporters involved in solute transportation across membranes via ATP hydrolysis were under-expressed in CLas-infected ACP to gain advantage of the membrane dysfunction. Suppression of the defense-related genes of ACP by CLas is consistent with the findings of Vyas et al.[3] Differential expression of a cell adhesion protein integrin, its binding protein talin and basal membrane formation protein papilin in CLas-infected ACP may mediate cell shape change during adhesion and invasion process as speculated by Das et al. and Vyas et al.[3,28]

Among the major metabolic pathways of ACP affected by CLas, carbohydrate, energy and nucleotide metabolism were important. To meet out the energy and nucleotide requirements, CLas manipulates the respective pathways of the vector.[29] Considering the non-metabolic pathways, endocytotic pathway plays an inevitable role in host invasion by CLas.[3] Enrichment of genes associated with cellular endocytosis in ACP suggests possible manipulation of endocytotic pathway upon CLas infection.

## 5 Conclusion

In conclusion, a total of 3911 genes were differentially expressed including 2196 up-regulated and 1715 down-regulated genes. Most DEGs included vitellogenins, extensin, cytoskeleton and endocytotic pathway-related genes. Molecular functions were highly enriched in CLas-infected ACP. Carbohydrate, energy, and nucleotide metabolism were the major metabolic pathways affected while endocytotic and defense-related pathways that facilitate the circulation and multiplication of CLas in ACP were also affected. The putative genes of ACP that are highly regulated in response to CLas can be targeted for the effective management of CLas once validated functionally.

## Acknowledgments

The sequencing service provided by Nucleome Informatics Pvt. Ltd. Hyderabad, India is thankfully acknowledged. We also acknowledged the support received from IARI, and DBT. The funding bodies played no role in the design of the study and collection, analysis, and interpretation of data and in writing the manuscript.

## Ethics approval and consent to participate

Not applicable

 doi:10.20944/preprints202005.0389.v1

**Consent for publication**

Not applicable

**Competing interest**

All authors declare that there are no conflicts of interest in regard to the work reported in this paper.

**Data availability**

The datasets generated during the current study are available in the NCBI with BioProject ID PRJNA634436.

**Funding**

Indian Agricultural Research Institute, New Delhi

Department of Biotechnology, Government of India

**Authors contributions**

AG and VKB conceived and designed the research. AG prepared biological samples. DJ and RR carried out the wet lab experiments. VKS analysed data. SKS provided HLB isolate. NC reviewed the results. DJ and VKS wrote draft manuscript. VKB and AG edited final manuscript. All authors read and approved the manuscript.

**References**

1. Bové JM. Huanglongbing: a destructive, newly-emerging, century-old disease of citrus. Journal of Plant Pathology. 2006; 88(1): 7-37.

2. Gottwald TR, Graça JVD, Bassanezi RB. Citrus huanglongbing: the pathogen and its impact. Plant Health Progress. 2007; 8(1): 31.

3. Vyas M, Fisher TW, He R, Nelson W, Yin G, Cicero JM, Willer M, Kim R, Kramer R, May GA, Crow JA, Soderlund CA, Gang DR, Brown JK. Asian citrus psyllid expression profiles suggest *Candidatus* Liberibacter asiaticus-mediated alteration of adult nutrition and metabolism, and of nymphal development and immunity. PLoS One. 2015; 10(6): e0130328.

4. Halbert SE, Manjunath KL. Asian citrus psyllids (Sternorrhyncha: Psyllidae) and greening disease of citrus: a literature review and assessment of risk in Florida. Florida Entomologist. 2004; 87(3): 330-353.

5. Wu Z, Zhang H, Bin S, Chen L, Han Q, Lin J. Antennal and abdominal transcriptomes reveal chemosensory genes in the Asian citrus psyllid, *Diaphorina citri.* PLoS One. 2016; 11(7):e0159372.

6. Bastianel C, Garnier-Semancik M, Renaudin J, Bové JM, Eveillard S. Diversity of "*Candidatus Liberibacter* asiaticus," based on the omp gene sequence. Applied and Environmental Microbiology. 2005; 71(11): 6473-6478.

7. Du Z, Zhou X, Ling Y, Zhang Z, Su Z. agriGO: a GO analysis toolkit for the agricultural community. Nucleic Acids Research. 2010; 38(suppl_2): W64-W70.

8. Bin S, Pu X, Shu B, Kang C, Luo S, Tang Y, Wu Z, Lin J. Selection of reference genes for optimal normalization of quantitative real-time polymerase chain reaction results for *Diaphorina citri* adults. Journal of Economic Entomology. 2019; 112(1): 355-363.

9. Livak KJ, Schmittgen TD. Analysis of relative gene expression data using real-time quantitative PCR and the $2^{-\Delta\Delta CT}$ method. Methods. 2001; 25(4): 402-408.

10. Ingwell LL, Eigenbrode SD, Bosque-Pérez NA. Plant viruses alter insect behavior to enhance their spread. Scientific Reports. 2012; 2: 578 https://doi.org/10.1038/srep00578.

11. Fiebig M, Poehling HM, Borgemeister C. Barley yellow dwarf virus, wheat, and Sitobion avenae: a case of trilateral interactions. Entomologia Experimentalis et Applicata, 2004; 110(1): 11-21.

12. Belliure B, Arne J, Maurice WS. Herbivore benefits from vectoring plant virus through reduction of period of vulnerability to predation. Oecologia. 2008; 156(4): 797-806.

13. Ghosh A, Das A, Vijayanandraj S, Mandal B. Cardamom bushy dwarf virus infection in large cardamom alters plant selection preference, life stages, and fecundity of aphid vector, *Micromyzus kalimpongensis* (Hemiptera: Aphididae). Environmental Entomology. 2016; 45(1): 178–184.

14. Ghosh A, Basavaraj YB, Jangra S, Das A. Exposure to watermelon bud necrosis virus and groundnut bud necrosis virus alters the life history traits of their vector, *Thrips palmi* (Thysanoptera: Thripidae). Archives of Virology. 2019; 164: 2799–2804.

15. Tufail M, Nagaba Y, Elgendy AM, Takeda M. Regulation of vitellogenin genes in insects. Entomological Science. 2014; 17(3): 269-282.

16. Piulachs MD, Guidugli KR, Barchuk AR, Cruz J, Simoes ZLP, Belles X. The vitellogenin of the honey bee, *Apis mellifera*: structural analysis of the cDNA and expression studies. Insect Biochemistry and Molecular Biology. 2003; 33(4), 459-465.

17. Nakamura A, Yasuda K, Adachi H, Sakurai Y, Ishii N, Goto S. Vitellogenin-6 is a major carbonylated protein in aged nematode, *Caenorhabditis elegans*. Biochemical and Biophysical Research Communications. 1999; 264(2): 580-583.

18. Seehuus SC, Norberg K, Gimsa U, Krekling T, Amdam GV. Reproductive protein protects functionally sterile honey bee workers from oxidative stress. Proceedings of the National Academy of Sciences. 2006; 103(4), 962-967.

19. Singh NK, Pakkianathan BC, Kumar M, Prasad T, Kannan M, König S, Krishnan, M. Vitellogenin from the silkworm, *Bombyx mori*: an effective anti-bacterial agent. PLoS One. 2013; 8(9): e73005.

20. Huo Y, Yu Y, Chen L, Li Q, Zhang M, Song Z, Chen X, Fang R, Zhang, L. Insect tissue-specific vitellogenin facilitates transmission of plant virus. PLoS pathogens. 2018; 14(2): e1006909.

21. Sinha DK, Chandran P, Timm AE, Aguirre-Rojas L, Smith CM. (2016). Virulent *Diuraphis noxia* aphids over-express calcium signaling proteins to overcome defenses of aphid-resistant wheat plants. PloS one. 2016; 11(1): e0146809.

22. de Almeida Dias F, dos Santos ALS, Lery LMS, e Silva TLA, Oliveira MM, Bisch PM, Saraiva EM, Souto-Padrón TC, Lopes AH. Evidence that a laminin-like insect protein mediates early events in the interaction of a Phytoparasite with its vector's salivary gland. PloS one. 2012; 7(10): e48170.

23. Goins LM, Mullins RD. A novel tropomyosin isoform functions at the mitotic spindle and Golgi in Drosophila. Molecular Biology of the Cell. 2015; 26(13): 2491-2504.

24. Lan H, Hong X, Huang R, Lin X, Li Q, Li K, Zhou T. RNA interference-mediated knockdown and virus-induced suppression of Troponin C gene adversely affect the behavior or fitness of the green rice leafhopper, *Nephotettix cincticeps*. Archives of insect biochemistry and physiology, 2018; 97(2): e21438.

25. Ramsey JS, Johnson RS, Hoki JS, Kruse A, Mahoney J, Hilf ME, Hunter WB, Hall DG, Schroeder FC, MacCoss MJ, Cilia M. Metabolic interplay between the Asian citrus psyllid and its *Profftella* symbiont: an Achilles' heel of the citrus greening insect vector. PLoS One. 2015; 10(11): e0140826.

 doi:10.20944/preprints202005.0389.v1

26. Barton B, Ayer G, Heymann N, Maughan DW, Lehmann FO, Vigoreaux JO. Flight muscle properties and aerodynamic performance of *Drosophila* expressing a flightin transgene. Journal of Experimental Biology. 2005; 208(3): 549-560.

27. Ghanim M, Fattah-Hosseini S, Levy A, Cilia M. Morphological abnormalities and cell death in the Asian citrus psyllid (*Diaphorina citri*) midgut associated with *Candidatus* Liberibacter asiaticus. Scientific Reports 2016; 6: 33418.

28. Das M, Ithychanda SS, Qin J, Plow EF. Mechanisms of talin-dependent integrin signaling and crosstalk. Biochimica Et Biophysica Acta. 2014; 1838(2): 579-588.

29. Killiny N, Hijaz F, Ebert TA, Rogers ME. A plant bacterial pathogen manipulates its insect vector's energy metabolism. Applied and Environmental Microbiology. 2017; 83(5): e03005-16.

Preprints (www.preprints.org) | NOT PEER-REVIEWED | Posted: 24 May 2020 doi:10.20944/preprints202005.0389.v1

**Table 1. List of primers used in this study for qRT-PCR analysis**

| Gene name | Primer sequences (5'-3') | Amplicon length (bp) | Reference |
|---|---|---|---|
| ***tropomyosin-1*** | F: GGGCAAGACGGAAGAAGGGTTTCA<br>R: TCGTCCGTGTCCTTGGGCTCT | 166 | This study |
| ***troponin C-like*** | F: TGGAGAGCTTGAGTTCAACGAGT<br>R: TCGTACAACATGAAGGCTTCGC | 114 | This study |
| ***vitellogenin-1-like*** | F: CCCAGACATGGAAACAACAGCCA<br>R: GGCATGGCCTTGGTACTGAAGCA | 195 | This study |
| ***vitellogenin-2-like*** | F: TGCCAACCACCCACAAGCTGA<br>R: TCCAGCGTAACGGGCGATTCT | 191 | This study |
| ***α-tubulin*** | F: GCTTTCCAACACCACCGCTAT<br>R: AGGTCTTCCCTCGCCTCTGA | 144 | Bin et al.[8] |

**Table 2. Summary of the Illumina sequencing and mapping of three transcript libraries**

| | P+CLas1 | P+CLas2 | P-CLas |
|---|---|---|---|
| **Total raw reads** | 77173334 | 65309914 | 63961850 |
| **Total clean reads** | 76545332 (99.19%) | 64792738 (99.21%) | 63274696 (98.93%) |
| **GC content** | 42.00% | 38.00% | 44.00% |
| **Total mapped reads** | 45066432 (58.88%) | 40693331 (62.81%) | 30603982 (48.37%) |
| **Multiple mapped reads** | 9087445 (11.87%) | 9939837 (15.34%) | 5831837 (9.22%) |
| **Uniquely mapped reads** | 35978987 (47.00%) | 30753494 (47.46%) | 24772145 (39.15%) |

Preprints (www.preprints.org) | NOT PEER-REVIEWED | Posted: 24 May 2020 doi:10.20944/preprints202005.0389.v1

**Table 3. Details of the top twenty upregulated and downregulated genes of ACP in response to CLas infection**

| Gene Id | $Log_2FC$ | $P_{adj}$ value | Regulation | Protein product | Protein name |
|---|---|---|---|---|---|
| LOC103523873 | 16.66216 | 4.54E-25 | Up | XP_008487105.1 | vitellogenin-1-like |
| LOC103523874 | 16.22512 | 7.80E-24 | Up | XP_008487106.1 | vitellogenin-1-like |
| LOC103513496 | 15.83361 | 1.00E-22 | Up | XP_008476553.1 | vitellogenin-1-like |
| LOC103513097 | 15.06717 | 1.62E-20 | Up | XP_008476127.1 | extensin-like |
| LOC103513510 | 14.70817 | 1.67E-19 | Up | XP_008476568.2 | vitellogenin-2-like |
| LOC103523201 | 14.55122 | 3.79E-19 | Up | XP_017304666.1 | vitellogenin-like, partial |
| LOC103523199 | 13.59177 | 2.01E-16 | Up | XP_008486485.1 | vitellogenin-like |
| LOC103511339 | 13.57851 | 2.08E-16 | Up | XP_008474281.2 | Extension |
| LOC103513507 | 13.49574 | 3.49E-16 | Up | XP_008476565.1 | vitellogenin-3-like |
| LOC103511254 | 13.38276 | 6.88E-16 | Up | XP_008474194.1 | cathepsin F-like |
| LOC103507356 | 13.32201 | 9.58E-16 | Up | XP_017298773.1 | extensin-like |
| LOC103523134 | 13.29403 | 1.11E-15 | Up | XP_008486427.1 | phosphoenolpyruvate carboxykinase, cytosolic |
| LOC108254328 | 13.26727 | 1.28E-15 | Up | XP_017304823.1 | vitellogenin-like, partial |
| LOC103513495 | 13.06968 | 4.76E-15 | Up | XP_008476552.1 | vitellogenin-1-like |
| LOC103523837 | 12.80216 | 2.75E-14 | Up | XP_017304824.1 | vitellogenin-like |
| LOC103521261 | 12.32291 | 5.17E-13 | Up | XP_008484592.1 | cathepsin L1-like |
| LOC103504974 | 12.32267 | 5.17E-13 | Up | XP_017305410.1 | uncharacterized protein |
| LOC103521262 | 12.19779 | 1.06E-12 | Up | XP_008484593.1 | cathepsin F-like |
| LOC103520524 | 12.05602 | 2.43E-12 | Up | XP_017304029.1 | uncharacterized protein, partial |
| LOC103516344 | 11.94178153 | 4.97E-12 | Up | XP_017302502.1 | mucin-5AC-like, partial |
| LOC103524036 | -8.10347 | 3.66E-29 | Down | XP_008487263.1 | myosin heavy chain, muscle-like |
| LOC103506300 | -8.07657 | 1.15E-31 | Down | XP_008468906.1 | troponin C-like |
| LOC103506299 | -7.80828 | 1.90E-30 | Down | XP_008468905.1 | uncharacterized protein |
| LOC103514141 | -7.27271 | 2.01E-27 | Down | XP_008477228.1 | tropomyosin-1, isoforms 33/34-like isoform X1 |
| LOC103512979 | -6.18095 | 3.79E-19 | Down | XP_008476010.1 | E3 ubiquitin-protein ligase HECW2-like, partial |
| LOC103508322 | -5.99975 | 1.62E-20 | Down | XP_008471095.1 | Flightin |

 doi:10.20944/preprints202005.0389.v1

| | | | | | |
|---|---|---|---|---|---|
| LOC103520593 | -5.95585 | 8.34E-18 | Down | XP_008483915.1 | nexilin-like, partial |
| LOC103506414 | -5.92598 | 2.49E-19 | Down | XP_008469022.1 | ankyrin repeat domain-containing protein 33B-like |
| LOC108252030 | -5.41842 | 8.05E-17 | Down | XP_017298349.1 | uncharacterized protein |
| LOC103519909 | -5.38056 | 8.91E-17 | Down | XP_008483253.1 | tubulin polyglutamylase TTLL6-like |
| LOC103519412 | -5.28662 | 1.68E-13 | Down | XP_017303679.1 | cathepsin B-like cysteine proteinase 6, partial |
| LOC103514143 | -5.26114 | 1.17E-16 | Down | XP_017301589.1 | dynein heavy chain 5, axonemal |
| LOC103519459 | -5.10164 | 7.11E-16 | Down | XP_017303780.1 | protein msta-like |
| LOC103508333 | -5.09911 | 1.61E-12 | Down | XP_017299199.1 | uncharacterized protein |
| LOC108253733 | -4.98455 | 5.19E-14 | Down | XP_017303753.1 | uncharacterized protein |
| LOC103519343 | -4.9033 | 3.25E-13 | Down | XP_008482653.1 | mpv17-like protein |
| LOC108253528 | -4.86711 | 8.28E-15 | Down | XP_017303150.1 | ejaculatory bulb-specific protein 3-like |
| LOC103505674 | -4.81176 | 2.18E-11 | Down | XP_008468252.2 | proteoglycan 4-like |
| LOC108253969 | -4.78468 | 2.52E-13 | Down | XP_017304321.1 | protein TonB-like |
| LOC108252773 | -4.71008 | 1.71E-10 | Down | XP_017300865.1 | uncharacterized, partial |

Preprints (www.preprints.org) | NOT PEER-REVIEWED | Posted: 24 May 2020 doi:10.20944/preprints202005.0389.v1

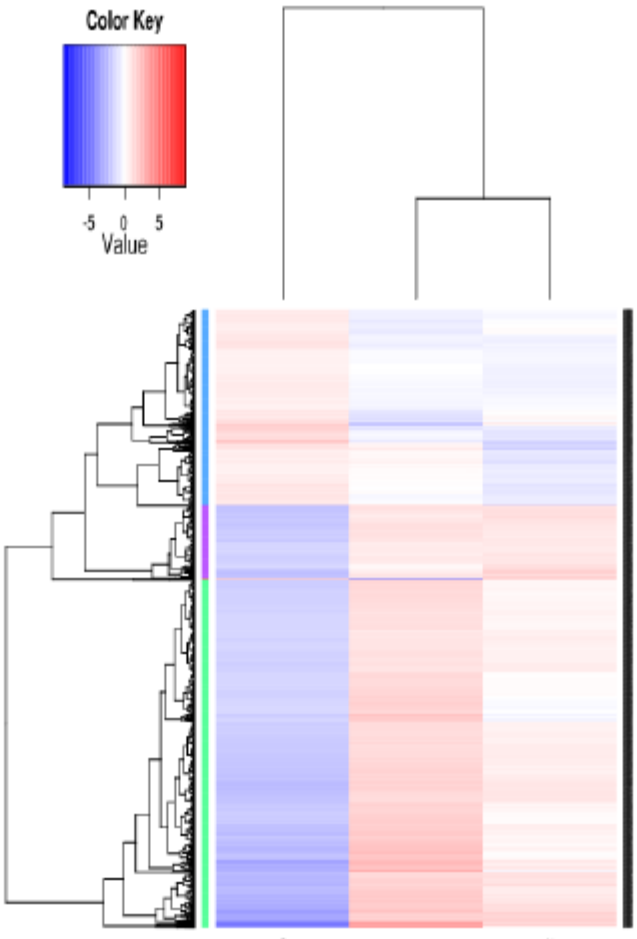


**Figure 1**

**The overall results of FPKM cluster analysis, clustered using the log2 (FPKM+1) value.** Red denotes genes with high expression levels, and blue denotes genes with low expression levels. The color range from blue to red represents the $\log_2$ (FPKM+1) value from large to small.

*Preprints* (www.preprints.org) | NOT PEER-REVIEWED | Posted: 24 May 2020 doi:10.20944/preprints202005.0389.v1

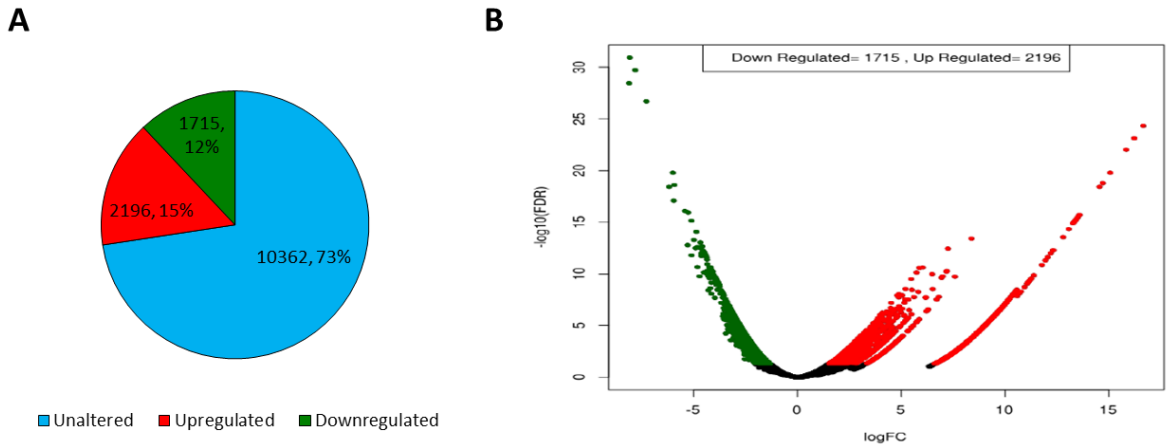


**Figure 2**

**Differential gene expression analysis. (A)** Proportion of differentially expressed genes in the total transcriptome. **(B)** Volcano plot for differentially expressed genes. The x-axis shows the fold change in gene expression between different samples, and the y-axis shows the statistical significance of the differences. Significantly up and down regulated genes are highlighted in red and green, respectively.

Preprints (www.preprints.org) | NOT PEER-REVIEWED | Posted: 24 May 2020 doi:10.20944/preprints202005.0389.v1

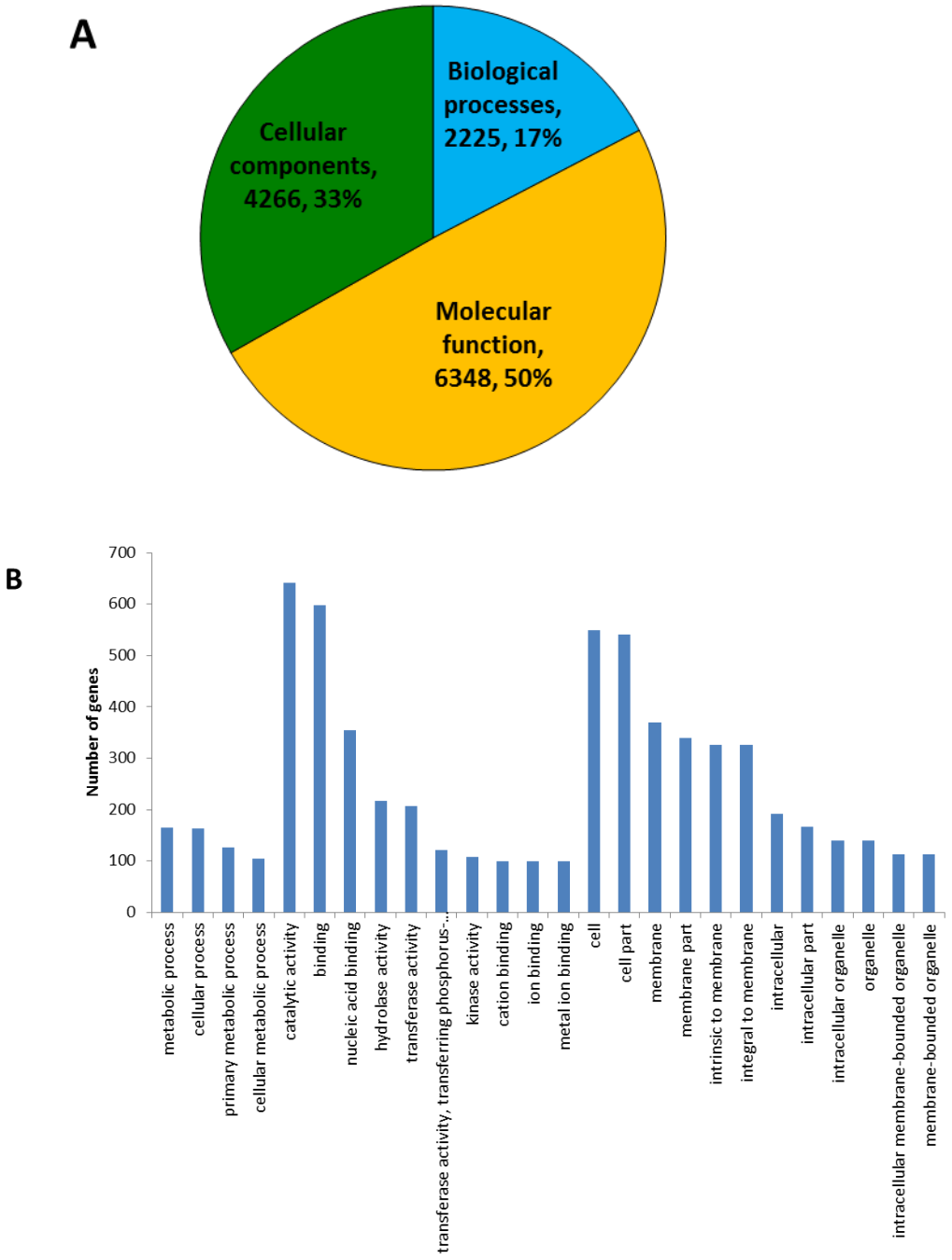


**Figure 3**

**GO Enrichment Analysis of DEGs. A.** Proportion of differentially expressed genes that participate in biological processes, cellular components and molecular functions. **(B)** Major processes and functions that are affected in CLas-infected *D. citri*.

*Preprints* (www.preprints.org) | NOT PEER-REVIEWED | Posted: 24 May 2020 doi:10.20944/preprints202005.0389.v1

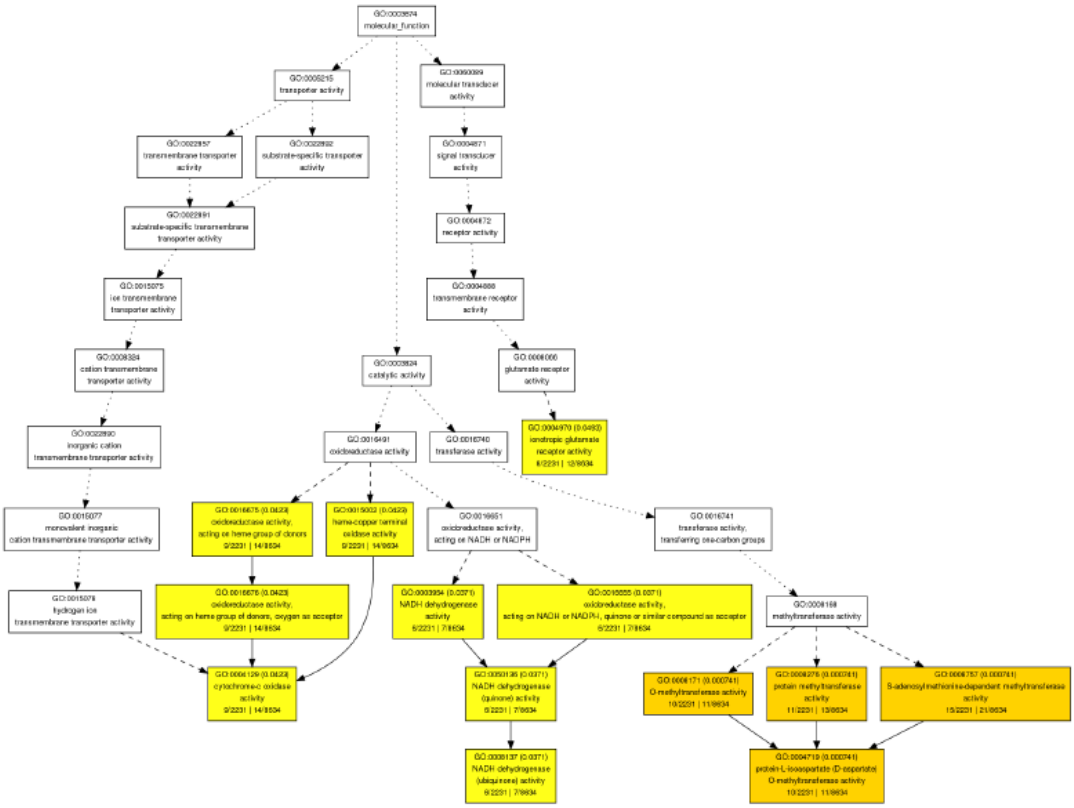


**Figure 4**

**Illustration of top GO DAG under molecular functions category.** Each node represents a GO term, the darker the color is, the higher is the enrichment level of the term. The name and p-value of each term are present on the node.

Preprints (www.preprints.org) | NOT PEER-REVIEWED | Posted: 24 May 2020 doi:10.20944/preprints202005.0389.v1

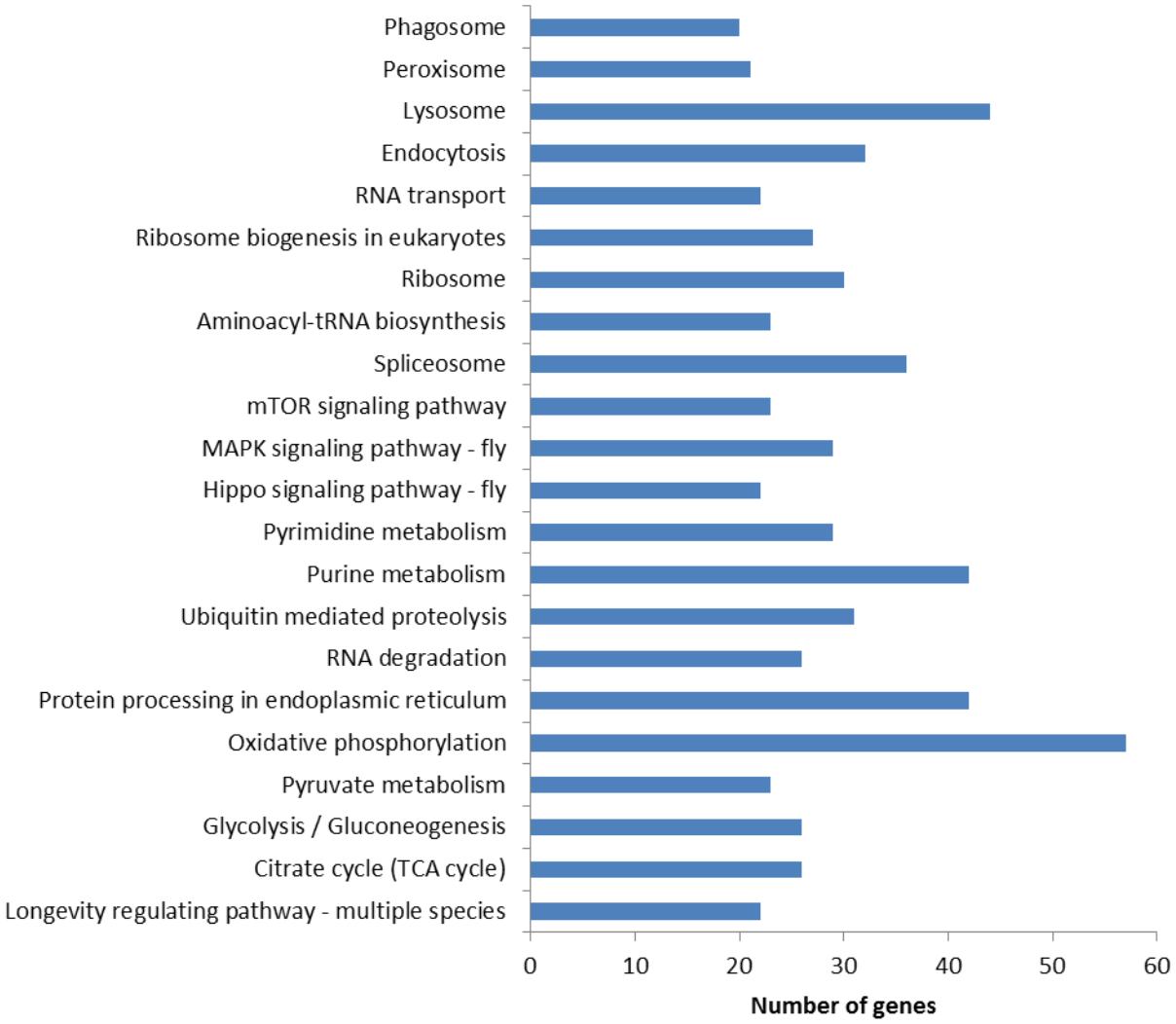


**Figure 5**
**KEGG pathway analysis of DEGs in *D. citri* upon Clas infection.** Major pathways affected in CLas infected *D. citri* are shown.

Preprints (www.preprints.org) | NOT PEER-REVIEWED | Posted: 24 May 2020 doi:10.20944/preprints202005.0389.v1

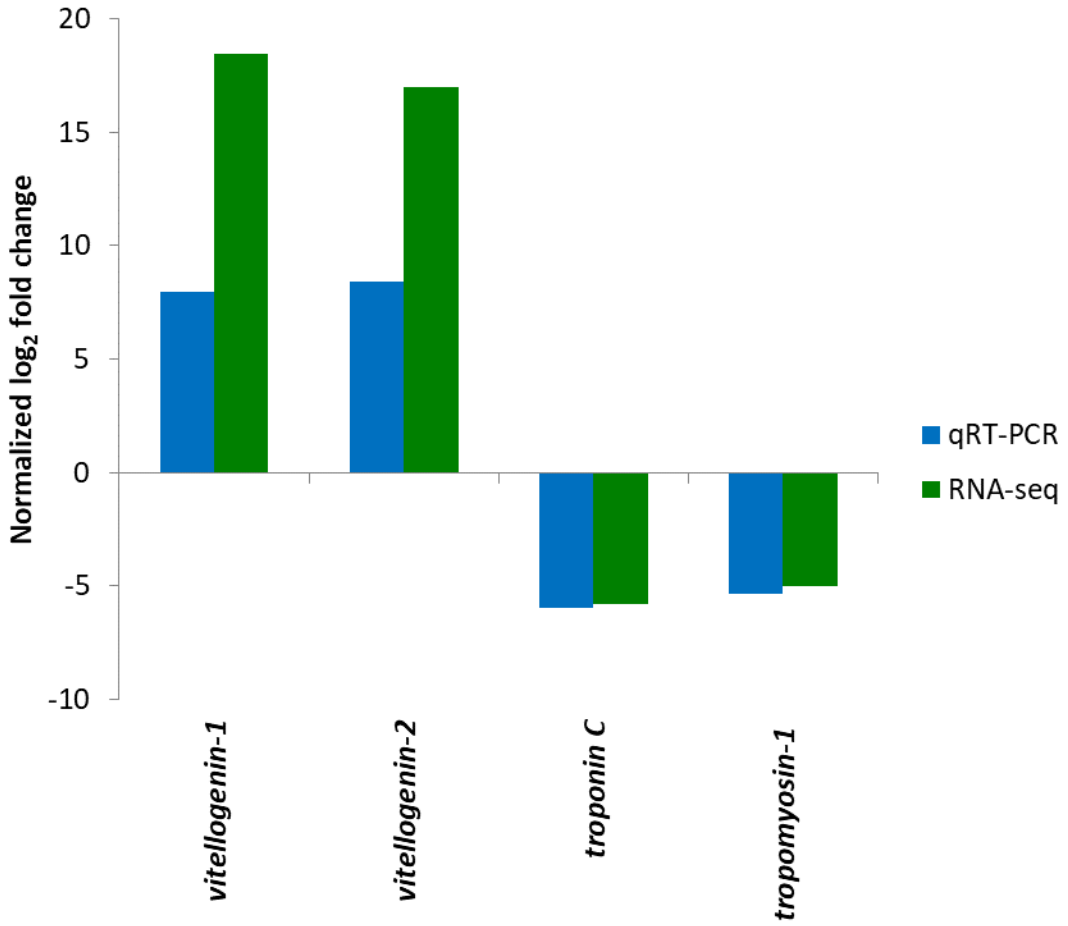


**Figure 6**
**Validation of the differential expression of selected genes related to insect cytoskeleton and nutrition using qRT-PCR.**